



Research Paper

SUPERLUMINAL SYNCHROTRON RADIATION

M.A. Aginian*, S.G. Arutunian, E.G. Lazareva, A.V. Margaryan

Yerevan Physics Institute,
Alikhanian Br. Str. 2, Yerevan, Armenia, 0036**Abstract**

To avoid complex computations based on wide Fourier expansions, the electromagnetic field of synchrotron radiation (SR) was analyzed using Lienard–Wiechert potentials in this work. The retardation equation was solved for ultrarelativistic movement of rotating charge at distances up to the trajectory radius. The radiation field was determined to be constricted into a narrow extended region with transverse sizes approximately the radius of trajectory divided by the particle Lorentz factor (characteristic SR length) cubed in the plane of trajectory and the distance between the observation and radiation emission point divided by the Lorentz factor in the vertical direction. The Lienard–Wiechert field of rotating charge was visualized using a parametric form to derive electric force lines rather than solving a retardation equation. The electromagnetic field of a charging point rotating at superluminal speeds was also investigated. This field, dubbed a superluminal synchrotron radiation (SSR) field by analogy with the case of a circulating relativistic charge, was also presented using a system of electric force lines. It is shown that SSR can arise in accelerators from «spot» of SR runs faster than light by outer wall of circular accelerator vacuum chamber. Furthermore, the mentioned characteristic lengths of SR in orbit plane and in vertical direction are less than the interparticle distances in real bunches in ultrarelativistic accelerators. It is indicating that this phenomenon should be taken into account when calculating bunch fields and involved at least into the beam dynamic consideration.

Key words: synchrotron radiation, Lienard–Wiechert, electrical field lines, superluminal, particle accelerator

1. Introduction

Rather than solving the retardation equation, electric field lines in special parametric form were used in this work to illustrate the SR field including the Coulomb term for completeness. The electromagnetic field of charging point rotating with speed exceed the speed of light is investigated. By analogy with the case of a circulating relativistic charge we call this electromagnetic field as SSR.

The theoretical prerequisites for theory and experimental design of the coherent radiation of electromagnetic waves by sources moving at speeds exceeding the speed of light in empty space were considered in [1]. Furthermore, superluminal light spots caused by circular rotation have been investigated [2, 3]. Superluminal radiation has been shown to occur in an electromagnetic field reflection from a rotating conducting cylinder [4, 5]. In [6, 7] examined a model when the boundary surface is crossed by an obliquely incident extended bunch of charged particles, then superluminal transition radiation is the result of interference of radiation emitted by many par-

* Corresponding author. Yerevan Physics Institute, Alikhanian Br. Str. 2, Yerevan, Armenia, 0036. E-mail address: agmery@mail.yerphi.am

ticles, and [8] examined superluminal electromagnetic pulses produced by obliquely incident X-rays.

This work therefore aims to estimate of a superluminal point-like charge moving on a circle. The SSR is also presented by a system of electric force lines in the same way as for SR. It is noted that the SSR can arise from «spot» of SR runs faster than light by the outer wall of circular accelerator vacuum chamber. It is also pointed out that the characteristic lengths of SR and SSR are less than the interparticle distances in real bunches in ultrarelativistic accelerators. It is indicating that this phenomenon should be taken into account when calculating bunch fields and involved at least into the beam dynamic consideration.

2. Synchrotron Radiation

Relativistic electrons rotating in a magnetic field produce SR. The spectral SR energy emitted by one electron can be calculated as follows [9–13]

$$\frac{d^2W}{d\Omega d\omega} = \frac{3r_0 mc}{4\pi^2} \gamma^2 \frac{\omega^2}{\omega_c^2} (1 + \gamma^2 \psi^2)^2 \times \left[K_{2/3}^2(x) + \frac{\gamma^2 \psi^2}{1 + \gamma^2 \psi^2} K_{1/3}^2(x) \right], \quad (1)$$

where ψ is the angle between the orbit plane and radiation detection direction, θ is angle of observation in the horizontal plane, $d\Omega = d\theta d\psi$, and ω is the angular frequency of a photon. The Lorentz factor of an electron γ is equal to the electron energy divided by $m_e c^2$, where m_e is the electron mass and c is the velocity of light. The electron classical radius is defined as $r_0 = e^2/m_e c^2$, $x = (\omega/2\omega_c)(1 + \gamma^2 \psi^2)^{3/2}$, the critical frequency that divides the emitted power into equal halves is $\omega_c = 3\gamma^3 c/2\rho_0$, where ρ_0 is the radius of the charge trajectory, and $K_{1/3}$ and $K_{2/3}$ are modified second-order Bessel functions. For ultrarelativistic equations, $\gamma \gg 1$, the distribution is very wide and involves harmonics up to a γ^3 order of charge circulating frequency, $\omega_0 = c\beta/\rho_0$, where $\beta = v/c$, where v is the velocity of the electron.

The radiation beam rotates together with an electron and is directed along the direction of the velocity with an angular spread of the order $\Delta\theta \simeq 1/\gamma \ll 1$.

Wide Fourier expansions are known to correspond to narrow spatial structures. For SR the pulse width has a duration of $\Delta t \simeq \gamma^3 \omega_0$, where $\omega_0 = eH/\gamma m_e$ is the orbiting frequency (H is magnetic field). Therefore, SR is dominated by frequency components in the range $\omega = \gamma^3 \omega_0$.

SR theory is based on Lienard–Wiechert potentials [14], which give the equations for electromagnetic field. Here, a circulating electron with constant velocity was considered in the coordinate system described in Fig. 1.

Here, a charge is circulating in a counter-clockwise direction and is placed at the top of the circle at time $t=0$. The unit vectors corresponding to position of the charge on the circle were: $\vec{e}_1(\Phi)$ – directed along the radius, $\vec{e}_2(\Phi)$ – along the charge velocity. Angle Φ was measured in the counter-clockwise direction, where $\Phi=0$ corresponds to \vec{y} direction for $\vec{e}_1(\Phi)$. The radius-vector of moving charge is written in form:

$$\vec{r}_0(t) = \rho_0 \vec{e}_1(\Phi), \quad (2)$$

$$\text{where } \Phi = \frac{\beta c}{\rho_0} t.$$

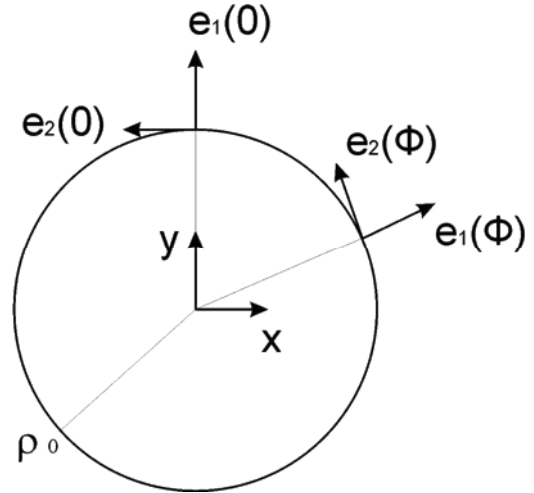


Fig. 1. Used coordinate system: r_0 is the radius of the charge trajectory, axes of laboratory coordinate system are denoted by x, y , unit vectors $\vec{e}_1(\Phi)$ and $\vec{e}_2(\Phi)$ are directed along radius and tangent to trajectory, angle Φ is counted out from y axis in counter-clockwise direction

The electric and magnetic fields of a circulating charge can be calculated as [6] follows:

$$\vec{E}(t) = e \left\{ \frac{\gamma^{-2} (\vec{n} - \vec{\beta})}{D^2 (1 - \vec{n}\vec{\beta})^3} + \frac{[\vec{n} \times [(\vec{n} - \vec{\beta}) \times d\vec{\beta}/dt']]}{cD(1 - \vec{n}\vec{\beta})^3} \right\}, \quad (3)$$

$$\vec{H}(t) = [\vec{n} \times \vec{E}], \quad (4)$$

where all values on the right side are taken at retardation time t' coupled with t by the retardation equation

$$c(t - t') = |\vec{r} - \vec{r}_0(t')| \quad (5)$$

and $D = c(t - t')$ in (3).

It should be noted that equations (3–5) formally solve the Maxwell equations for point-like charge moving with speed exceed the speed of light.

Since 1979, Lienard–Wiechert fields have been investigated by solving the retardation equation near the charge but far from the Coulomb area [15, 16].

The fields in the SR areas were estimated as done previously [17], where radius-vector of the observation point is described as:

$$\vec{r} = \rho_0(1 + \delta)\vec{e}_1(\Phi) + \rho_0\zeta\vec{e}_3, \quad (6)$$

where $\vec{e}_3 = [\vec{e}_1(\Phi) \Psi \vec{e}_2(\Phi)]$, and Φ , δ , and ζ represent the angular, radial, and vertical shifts in unit of radius from the charge position in the observation time. By expansion of parameter $\chi = (\Phi + \beta c(t-t')/\rho_0)/2$ over small values of γ^2 , Φ , δ , ζ , $c(t-t')/\rho_0$, the corresponding retardation equation was found to be as follows:

$$\chi^4 + 3\chi^2(\gamma^2 - \delta) - 3\chi\Phi + 3(\Phi^2 - \delta^2 - \zeta^2)/4 = 0. \quad (7)$$

SR is concentrated in the area defined by the simultaneous position of light signals emitted at retarded times along the direction of the charge velocity. Light signals emitted exactly in this direction along the velocity in retardation points form a line \vec{r}_γ . Near the charge, this line can be described by the equation which is as follows:

$$\vec{r}_\gamma(\Phi) = \rho_0(1 + (3\Phi)^{2/3}/2)\vec{e}_1(\Phi). \quad (8)$$

The observation points near the line \vec{r}_γ can be described using the angular shift φ normalized by the typical value of SR area angular width γ^3 by following expression:

$$\varphi = (\Phi - (2\delta)^{3/2}/3)\gamma^3. \quad (9)$$

Substituting this value into the retardation equation (7) provides an expression for χ which is as follows:

$$\chi = \sqrt{\delta/2} + \eta, \quad (10)$$

where $\eta = (\sqrt{9\varphi^2 + 1} + 3\varphi)^{1/3} - (\sqrt{9\varphi^2 + 1} - 3\varphi)^{1/3}$.

This provides the corresponding expressions for the electric and magnetic fields in the SR area:

$$\frac{\rho_0^2}{e} \vec{E} = \frac{2\sqrt{2}\gamma^4(1-\eta^2)}{(1+\eta^2)^3} \left\{ \frac{\vec{e}_1(\Phi)}{\delta^{1/2}} - \sqrt{2}\vec{e}_2(\Phi) \right\}, \quad (11)$$

$$\frac{\rho_0^2}{e} \vec{H} = -\frac{2\sqrt{2}\gamma^4(1-\eta^2)\vec{e}_3}{(1+\eta^2)^3}. \quad (12)$$

The main factor $2\sqrt{2}(1-\eta^2)/(1+\eta^2)^3$ is presented in Fig. 2 as a function of the angular (longitudinal) shift φ of the observation point from \vec{r}_γ .

Electric field lines were used to illustrate the field of SR. The first complete formula was obtained in [18]. Rather than solving the transcendental retardation equation, a parametric line can be introduced:

$$\vec{L}(t, t') = \rho_0\vec{e}_1\left(\frac{\beta c}{\rho_0}(t-t')\right) + c(t-t')\left(n_1\vec{e}_1\left(\frac{\beta c}{\rho_0}(t-t')\right) + n_2\vec{e}_2\left(\frac{\beta c}{\rho_0}(t-t')\right) + n_3\vec{e}_3\right). \quad (13)$$

One can see that observation point described by equation (13) and radius-vector of charge at retardation time t' are coupled by retardation equation (5) by definition.

For simplification, the dimensionless parameters as follows: $\tau = ct/\rho_0$, $\sigma = ct'/\rho_0$ were introduced, allowing (2) and (12) to be rewritten as:

$$\vec{r}_0(\tau)/\rho_0 = \vec{e}_1(\beta\tau), \quad (14)$$

$$\vec{L}(\tau, \sigma)/\rho_0 = \vec{e}_1(\beta(\tau-\sigma)) + (\tau-\sigma)(n_1\vec{e}_1(\beta(\tau-\sigma)) + n_2\vec{e}_2(\beta(\tau-\sigma)) + n_3\vec{e}_3), \quad (15)$$

where n_1 , n_2 , and n_3 are projections of unit vector \vec{n} along $\vec{e}_1(\beta(\tau-\sigma))$, $\vec{e}_2(\beta(\tau-\sigma))$ and \vec{e}_3 , respectively.

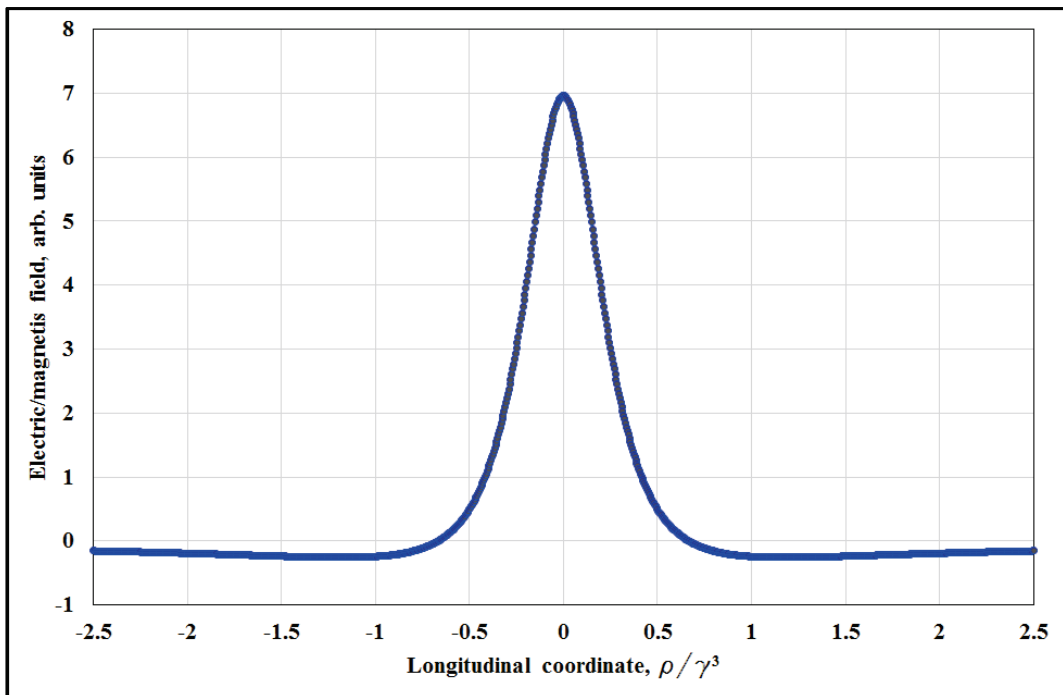


Fig. 2. Electromagnetic field in area of synchrotron radiation (SR) concentration

Parameters n_1 , n_2 , and n_3 are found from the condition that the derivation of (15) on $\tau-\sigma$ is directed along the electric field that gives following expressions:

$$n_1 = -\frac{\sqrt{1-c_2^2} \sin(\beta\gamma(\tau-\sigma) + c_1)}{\gamma(1 + \beta\sqrt{1-c_2^2} \cos(\beta\gamma(\tau-\sigma) + c_1))}, \quad (16)$$

$$n_2 = \frac{\beta + \sqrt{1-c_2^2} \sin(\beta\gamma(\tau-\sigma) + c_1)}{1 + \beta\sqrt{1-c_2^2} \cos(\beta\gamma(\tau-\sigma) + c_1)}, \quad (17)$$

$$n_3 = \frac{c_2}{\gamma(1 + \beta\sqrt{1-c_2^2} \cos(\beta\gamma(\tau-\sigma) + c_1))}, \quad (18)$$

where $-\pi \leq c_1 \leq \pi$ and $-1 \leq c_2 \leq 1$ are integration constants. One can see that these ranges of constants cover all initial directions of electric lines outgoing from the charge.

Transformation equations were then used to present the results in x and y coordinates which are as follows:

$$\bar{e}_1(\beta\sigma) = -\sin(\beta\sigma)\hat{x} + \cos(\beta\sigma)\hat{y}, \quad (19)$$

$$\bar{e}_2(\beta\sigma) = -\cos(\beta\sigma)\hat{x} - \sin(\beta\sigma)\hat{y}, \quad (20)$$

where \hat{x} , \hat{y} are unit vectors along the x and y axis, respectively, as in Fig. 1.

Illustrations of SR electric field lines for orbit plane are presented in Figs. 3 and 4. The shape and density of these lines describe the SR spatial structure. Thus, one can see the concentration of electric field lines stretched along the particle trajectory radius with transversal sizes strongly depend on charge energy.

To separate the area of SR concentration, the γ -region was introduced as a domain placed between the lines of signals emitted with angles $\pm\gamma'$ relative to particle speed. The electrical lines of SR in the γ -region are presented in Fig. 5

For relativistic particles the surfaces on which the spot of γ -region is running with linear velocity equal to speed of light and other one on which this spot is running with velocity more than speed of light are placed near the charge trajectory. Corresponding projections of charge trajectory on these surfaces we call luminal and superluminal trajectories (see Fig. 6 for $\gamma=50$).

The γ -region when $\gamma=7$ on the scale of orbit is presented in Fig. 7.

On the outer wall of vacuum chamber, the «spot» of SR is rotating with angular velocity $\omega=\beta c/\rho_0$ equal to angular velocity of circulating charge. When the distance between the charge trajectory and the outer wall of the vacuum chamber is $\delta\rho_0$ then the linear ve-

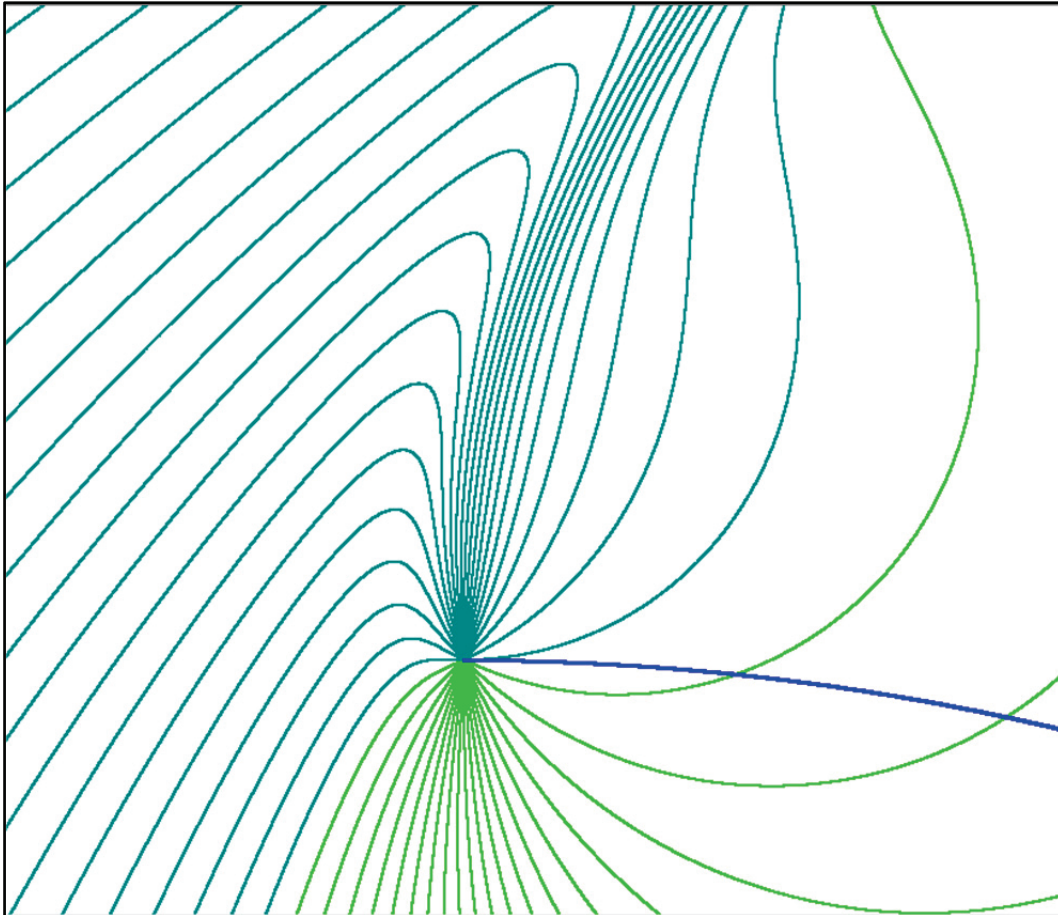


Fig. 3. Electrical field lines of SR when $\gamma=3$. One can see how these lines concentrate in space highlighting the SR

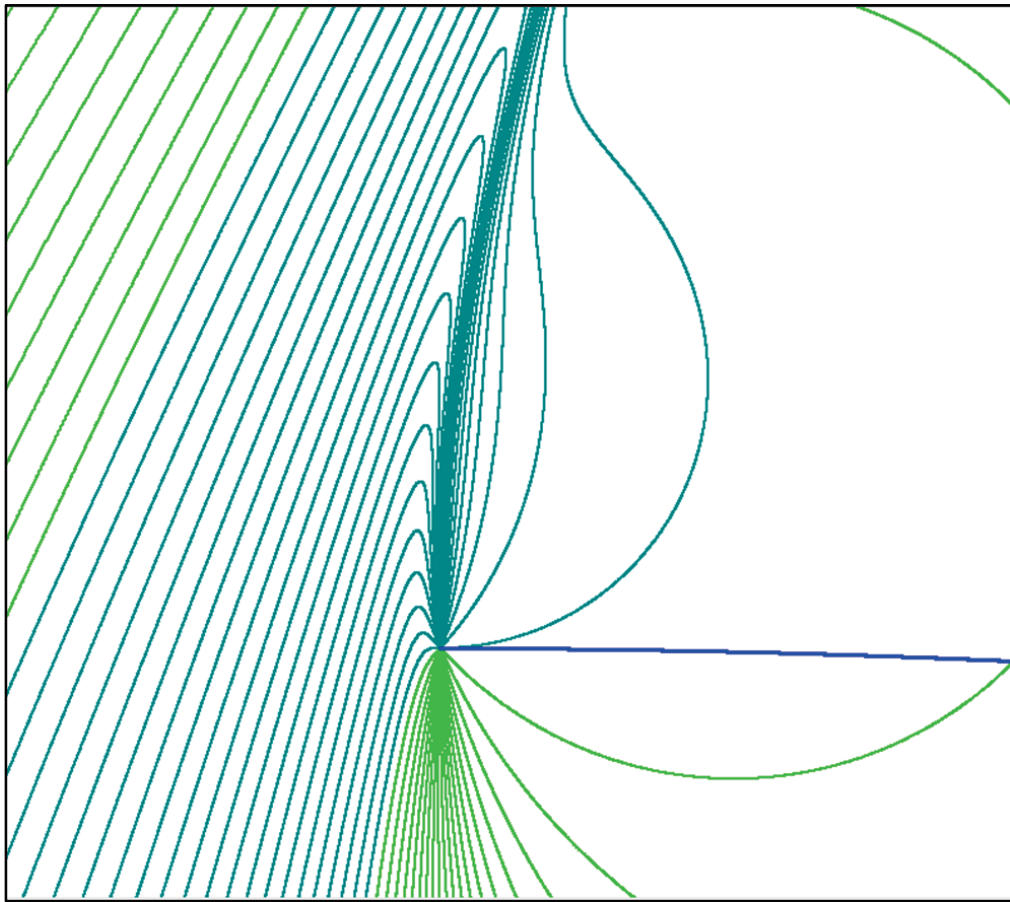


Fig. 4. Electrical field lines of SR when $\gamma=7$. The area of SR concentration is separated out. Scale factor of picture relative to Fig. 3 is 5

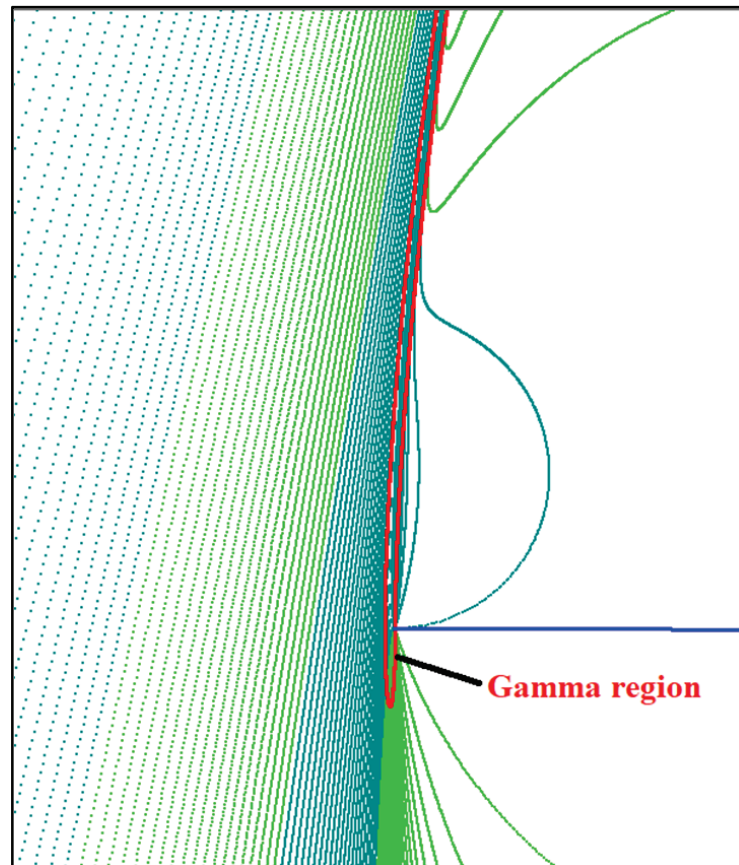


Fig. 5. Electrical field lines and γ -region of SR when $\gamma=20$. Scale factor of picture relative to Fig. 3 is 25

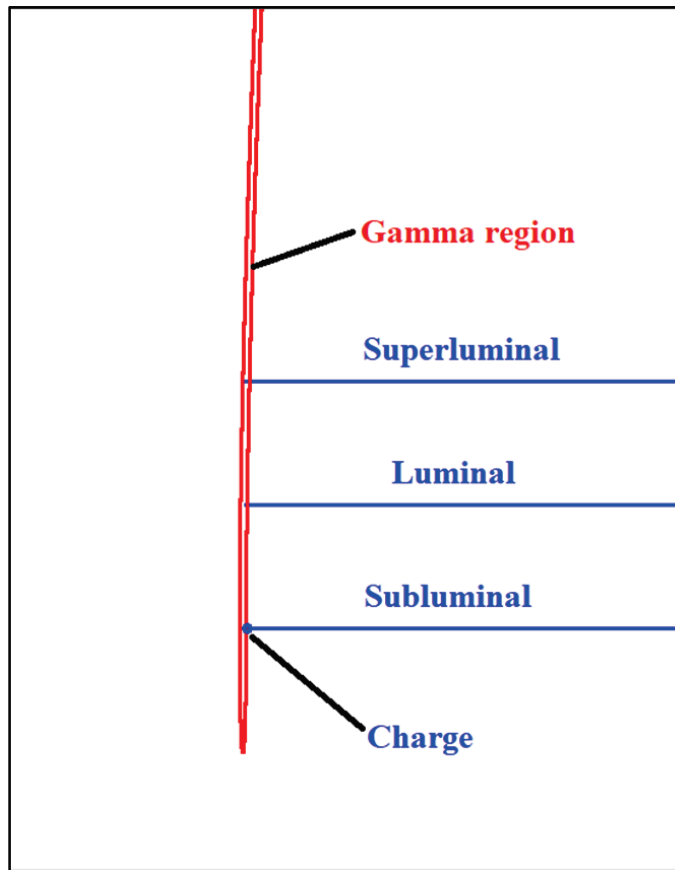


Fig. 6. The γ -region for $\gamma=50$. From bottom to top: trajectory of particle emitting the SR (subluminal trajectory), luminal trajectory corresponding to circle with linear velocity equal to velocity of light, and superluminal trajectory that is wall of vacuum chamber on which this spot is running with velocity more than speed of light. Scale factor of picture relative to Fig. 3 is 250

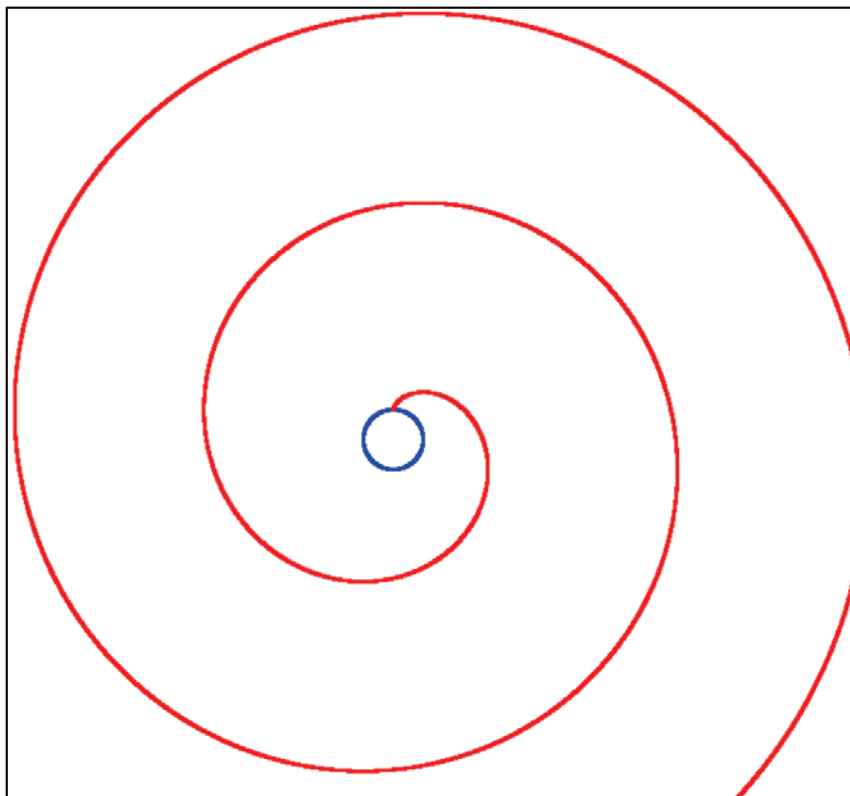


Fig. 7. The γ -region when $\gamma=7$ in scale of particle trajectory (blue). This is an area in which the SR concentrated into the space. Scale factor of picture relative to Fig. 3 is 0.0125

locity of the «spot» is equal to $\beta c(1+\delta)$. For typical values of synchrotron light sources $\beta c(1+\delta)$ is greater than for very small values of δ . E.g. for the CANDLE project [19] $E=3$ GeV ($\gamma=5.87E+03$) and radius of the trajectory in dipole magnet $\rho_0=7.4$ m (which corresponds to magnetic field $H=1.35$ T) the distance $\delta\rho_0$ at which velocity of «spot» exceed the speed of light is only 0.5 μm . Therefore, the SR spots move along the outer wall of the vacuum chamber faster than the speed of light.

The size of one spot is $S=(\rho_0/\gamma^3)(\rho_0\sqrt{\delta}/\gamma)$, where parameter δ depends on distance of particle to the wall. As the electric field in this area was directed along the radius, i.e., perpendicular to the wall surface, (11) and (12) could be used for field calculations. For a wall with ideal conductivity, the induced charge is calculated as:

$$q = -\sigma_e S, \quad (21)$$

where σ_e is the surface charge density equal to the magnitude of the electric field. Applying (11),

$$q \sim -\frac{e}{\rho_0^2} \frac{\gamma^4}{\sqrt{\delta}} \times \frac{\rho_0}{\gamma^3} \times \frac{\rho_0\sqrt{\delta}}{\gamma} = -e. \quad (22)$$

To estimate how the limit of the wall's conductivity decreases this value, a simple estimation of the charge displacement Δx was done as by [20] via the action of an electric field E :

$$\Delta x \approx (eE/m)\Delta t^2, \quad (23)$$

where $\Delta t = \rho_0/c\gamma^3$ is the SR acting time. Using (11), the following estimation can be obtained:

$$\Delta x \approx r_0 \frac{\gamma^{-2}}{\sqrt{\delta}}. \quad (24)$$

Induced by this displacement of all electrons of media with density n_e from the charged nuclei, electrical field is written as

$$E_m \approx en_e \times \Delta x = \frac{en_e r_0}{\sqrt{\delta}} \gamma^{-2}, \quad (25)$$

which is about $n_e r_0 \rho_0^2 \gamma^{-6}$ of the SR field magnitude and can be treated as correspondingly decreasing of wall conductivity. The CANDLE project found $n_e r_0 \rho_0^2 \gamma^{-6}$ to be approximately $3.2 \cdot 10^{-7}$ (for $n_e = 29.8.5 \cdot 10^{28} \text{ m}^{-3}$ copper value), indicating that the charge induced in a SR spot for one radiating electron is about $9.3 \cdot 10^{-6} e$. We assumed that all electrons in copper for corresponding frequencies are free.

3. Superluminal Synchrotron Radiation

This work aims to estimate electric field lines of a superluminal point-like charge moving with angular velocity ω_0 on a circle of radius ρ .

A point-like charge was assumed to be induced by a reference charge moving on a concentric circle of radius ρ_0 . For a superluminal charge trajectory $\rho^*(\tau)$

and retardation line $\vec{L}^*(\tau)$ attached to this trajectory, this indicates the following:

$$\frac{\vec{r}^*(\tau)}{\rho_0} = \eta \vec{e}_1 \left(\frac{B\tau}{\eta} + \Phi_0 \right), \quad (26)$$

$$\begin{aligned} \frac{\vec{L}^*(\tau, \sigma)}{\rho_0} = & \eta \vec{e}_1 \left(\frac{B(\tau - \sigma)}{\eta} + \Phi_0 \right) + \\ & + (\tau - \sigma) \left[\begin{aligned} & n_1 \vec{e}_1 \left(\frac{B(\tau - \sigma)}{\eta} + \Phi_0 \right) + \\ & + n_2 \vec{e}_2 \left(\frac{B(\tau - \sigma)}{\eta} + \Phi_0 \right) \end{aligned} \right], \end{aligned} \quad (27)$$

where $\eta = \rho/\rho_0$, $\tau = ct/\rho_0$, $\sigma = ct'/\rho_0$, and $B = \eta\beta = \eta\sqrt{1-\gamma^2} > 1$, assuming that at time $t=0$ a superluminal charge is placed on angle Φ_0 . The electrical field on line (27) according to (3) can be rewritten as:

$$\begin{aligned} \vec{E} = & \frac{e(1-B^2)}{D^2(1-Bn_2)^3} \times \\ & \times \left\{ \begin{aligned} & \left[n_1 + \frac{\Theta B^2}{\eta(1-B^2)}(1-Bn_2 - n_1^2) \right] \vec{e}_1 + \\ & + \left[(n_2 - B) \left(1 - \frac{\Theta B^2}{\eta(1-B^2)} n_1 \right) \right] \vec{e}_2 \end{aligned} \right\}, \end{aligned} \quad (28)$$

where $\Theta = \tau - \sigma$, $D = \rho_0(\tau - \sigma)$, and $\vec{e}_{1,2} = \vec{e}_{1,2} \left(\frac{B(\tau - \sigma)}{\eta} + \Phi_0 \right)$.

Calculating the derivation of (27) on Θ we find the tangents on these line at fixed observation time t :

$$\begin{aligned} \frac{d\vec{L}^*}{\rho_0 d\Theta} = & \\ = & (n_1 + \Theta \left(\frac{dn_1}{d\Theta} + n_2 \beta \right)) \vec{e}_1 + \Theta (n_2 - \beta + \left(\frac{dn_2}{d\Theta} - n \beta \right)) \vec{e}_2. \end{aligned} \quad (29)$$

Compare this equation with (28) we find the differential equations for n_1 and n_2 :

$$\eta \frac{dn_1}{d\Theta} = n_2(1 - Bn_2) \frac{B}{B^2 - 1}, \quad (30)$$

$$\eta \frac{dn_2}{d\Theta} = -n_1(1 - Bn_2) \frac{B}{B^2 - 1}. \quad (31)$$

One solution of these equations is presented as:

$$n_1^p = -\frac{\sinh(BG(\tau - \sigma)/\eta) + c_p)}{G(1 + B \cosh(BG(\tau - \sigma)/\eta) + c_p)}, \quad (32)$$

$$n_2^p = \frac{B + \cosh(BG\sigma + c_p)}{1 + B \cosh(BG\sigma + c_p)}, \quad (33)$$

where $G = 1/\sqrt{B^2 - 1}$ and the integration constant $-\infty < c_p < +\infty$. One can see that initial directions of unit vectors with components n_1 and n_2 outgoing from charge cover only angle $\pm \arccos(1/B)$ according ve-

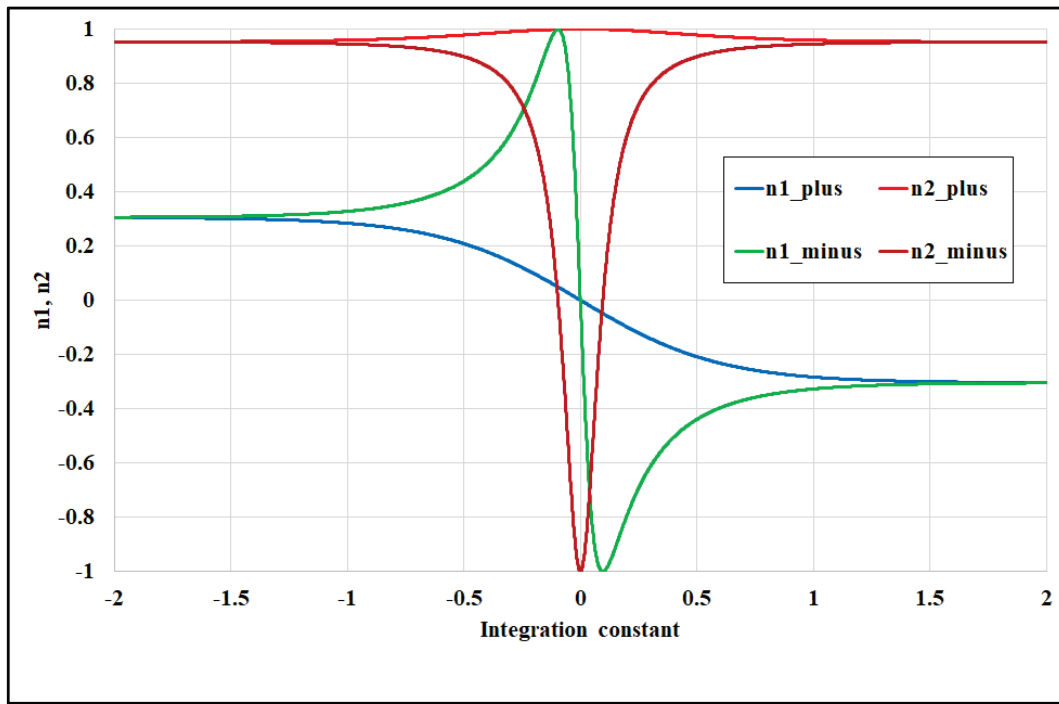


Fig. 8. Dependence of components of unit vector of electric line outgoing from the superluminal charge: $n1_plus$, $n2_plus$ for «plus» solution (32–33) and $n1_minus$, $n2_minus$ for «minus» solution (34–35) on integration constant

locity of the charge (we mark this solution as «plus» according to sign in denominator).

To cover other directions one can obtain the «minus» solution in form:

$$n_1^M = \frac{\sinh(BG(\tau - \sigma) / \eta) + c_M}{G(1 - B \cosh(BG(\tau - \sigma) / \eta) + c_M)}, \quad (34)$$

$$n_2^M = \frac{B - \cosh(BG(\tau - \sigma) / \eta) + c_M}{1 - B \cosh(BG(\tau - \sigma) / \eta) + c_M}, \quad (35)$$

where the integration constant $-\infty < c_M < +\infty$. Both solutions cover all possible initial directions of electric lines outgoing from the charge (see Fig. 8).

One can see that solutions (32–33) and (34–35) for electric lines are separated in space by surface given by a condition $\vec{n}\vec{B}=1$ known as Mach surface. As lead from (28) the field on the Mach surface goes to infinity.

The electric lines resulting from (27, 32–35) are shown in Figs. 9 and 10.

4. Discussion

This work aims to emphasize the fine spatial structure of SR. Vacuum chamber, especially the outer walls contribute to beam self-produced field a lot of faster than lights moving «spots.» The structure of the fields is so fine that for real bunches in accelerators it is thinner than interparticle distances, indicating that these effects should be involved at least in dynamic consideration. The issue will be interesting also for coherent SR investigation [21, 22].

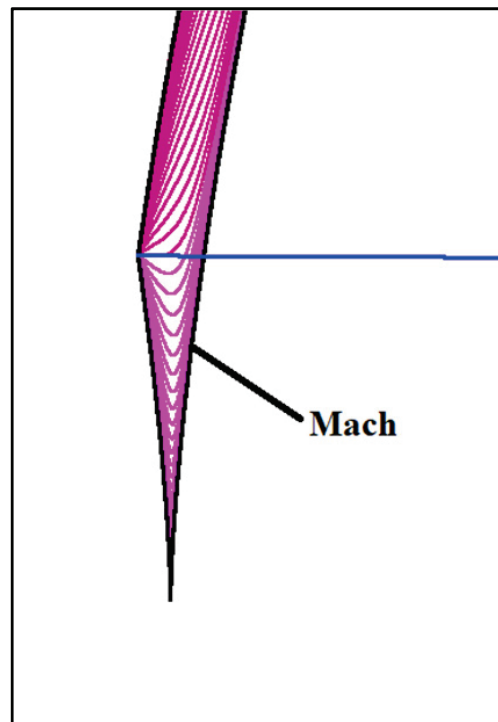


Fig. 9. Superluminal trajectory, $G=7$. Set of «plus» lines for all $-1 \leq c_i \leq 1$ (solution (32–33)) and Mach surface projection in orbit plane. This set of lines completely enclosed in the Mach surface. Scale factor of picture relative to Fig. 3 is 12.5

Acknowledgement

The work is devoted to the eightieth anniversary of the birth of Garry Nagorsky and memory of Andrey Amatuni.

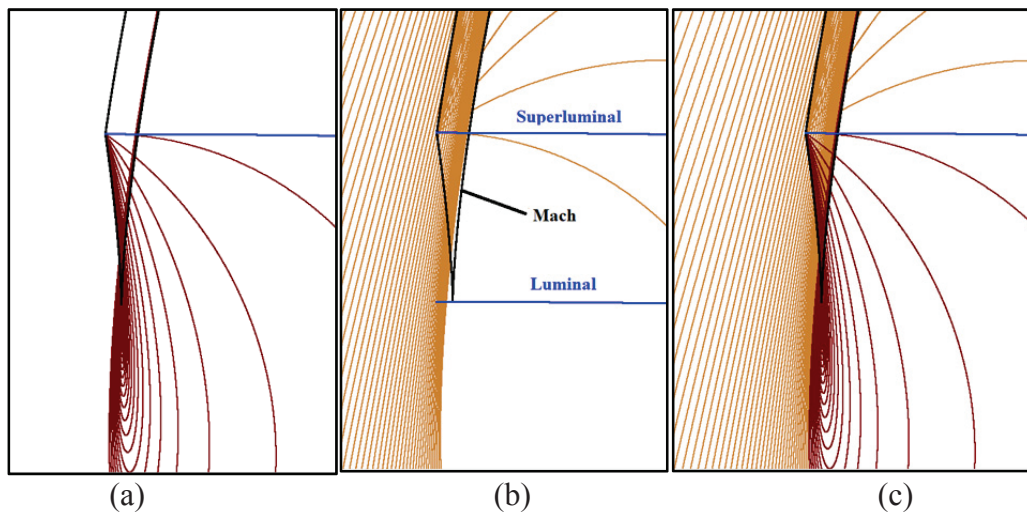


Fig. 10. Superluminal trajectory, $G=7$. a) Set of «minus» lines (solution (34–35)) for $-0 \leq c_l \leq 5$ and Mach surface projection in orbit plane. b) Set of «minus» lines (solution (34–35)) for $-5 \leq c_l \leq 0$ and Mach surface projection in orbit plane. The «beak» of «plus» branch of Mach surface lies on the luminal trajectory, where the velocity of linear propagation is equal to velocity of light, and the field reaches its maximum. c) Set of «minus» and «plus» lines (34–35) for $-5 \leq c_l \leq 0$ and Mach surface projection in orbit plane. Scale factor of picture relative to Fig. 3 is 12.5

References

- [1] Bolotovskiy B.M., Serov A.V. Radiation of superluminal sources in empty space. *Physics-Uspokhi*, 2005, vol. 48, no. 9, pp. 903–915. doi: 10.1070/PU2005v048n09ABEH002568.
- [2] Ginzburg V.L. On the Vavilov-Cherenkov effect and the anomalous Doppler effect in a medium in which the phase velocity of the waves is greater than the speed of light in a vacuum. *Journal of Experimental and Theoretical Physics*, 1972, vol. 62, no. 1, p. 176.
- [3] Bolotovskiy B.M., Ginzburg V.L. The Vavilov-Cherenkov Effect and the Doppler Effect in the Motion of Sources with Superluminal Velocity in Vacuum. *Physics-Uspokhi*, 1972, vol. 106, p. 577. doi: 10.1070/PU1972v015n02ABEH004962.
- [4] Zel'Dovich Ya. B. Generation of Waves by a Rotating Body. *Journal of Experimental and Theoretical Physics Letters*, 1971, vol. 14, p. 180.
- [5] Zel'Dovich Ya. B. Amplification of Cylindrical Electromagnetic Waves Reflected from a Rotating Body. *Soviet Physics JETP*, 1972, vol. 35, no. 6, pp. 1085–1087.
- [6] Bolotovskiy B.M., Serov A.V. Transition radiation excited by an extended system of charges, *JETP*, 2002, vol. 72, no. 1, p. 3.
- [7] Bolotovskiy B.M. On the radiation of a charged filament obliquely falling on an ideally conducting plane. *Short Reports on Physics (7)*, P. N. Lebedev Physical Institute of the Russian Academy of Sciences, 1972, p. 34.
- [8] Carron N.J., Longmire C.L. Electromagnetic pulse produced by obliquely incident X-rays. *IEEE Trans. Nucl. Sci.*, 1977, vol. NS-23, no. 6, pp. 1897–1902. doi: 10.1109/TNS.1976.4328596.
- [9] Wiedemann H. *Particle Accelerator Physics*, third ed. Berlin, Springer-Verlag Heidelberg, 2007, 948 p. doi: 10.1007/978-3-540-49045-6.
- [10] Kim K.-J. X-Ray Data Booklet. Available at: http://xdb.lbl.gov/Section2/Sec_2-1.html.
- [11] Mobilio S., Boscherini F., Meneghini C. *Synchrotron Radiation: Basics, Methods and Applications*, ed., Berlin, Springer, Springer-Verlag Heidelberg, 2015, 824 p. doi: 10.1007/978-3-642-55315-8.
- [12] Rivkin L. Electron dynamics with Synchrotron Radiation. Available at: <https://indico.cern.ch/event/279729/contributions/1626389/attachments/512375/707123/ElectronDynamicsLRivkin.pdf>.
- [13] Hofmann A. *The Physics of Synchrotron Radiation*, New York, Cambridge University Press, 2004, 348 p.
- [14] Landau L.D., Lifshitz E.M. *The Classical Theory of Fields*, New York, Pergamon Press, 1972, 374 p.
- [15] Arutyunyan S.G. Simultaneous picture of a field near an ultrarelativistic charged particle moving in a circle. Yerevan, EFI-387(45)-79, 1979, 19 p. In Russian.
- [16] Arutyunyan S.G. Electromagnetic field lines of a point charge moving arbitrarily in vacuum. *Physics-Uspokhi*, 1986, vol. 29, no. 11, pp. 1053–1057.
- [17] Arutyunyan S.G., Nagorsky G.A. Coherent addition of fields of relativistic charged particles moving along curvilinear trajectories. *Technical Physics Journal*, 1985, vol. 55, no. 8, pp. 1494–1499.
- [18] Aginian M.A., Arutunian S.G. Force lines of electric and magnetic fields of an arbitrarily moving charge. *Radiophysics and Quantum Electronics*, 1985, vol. 28, no. 7, pp. 619–624.
- [19] CANDLE Design Report, July 2002. Available at: http://candle.am/wp-content/uploads/2015/04/ACK_L.pdf.
- [20] Jackson J.D. *Classical Electrodynamics*, third ed., New York, Wiley, 1999, 791 p. doi: 10.1119/1.19136.
- [21] Novokhatski A. Modeling of Coherent Synchrotron Radiation Using a Direct Numerical Solution of Maxwell's Equations, 2012, Proc. of ICAP2012, Germany, Rostock-Warnemünde, pp. 107–111.
- [22] Novokhatski A. Coherent Synchrotron Radiation: Theory and Simulations, SLAC-PUB-14893, 2012. Available at: <http://www.slac.stanford.edu/cgi-wrap/getdoc/slac-pub-14893.pdf>.

Received 18.07.2018